Int. J. Heat Mass Transfer. Vol. 18, pp. 1149–1159. Pergamon Press 1975. Printed in Great Britain

COMPOSITE HEAT TRANSFER IN A PIPE WITH THERMAL RADIATION OF TWO-DIMENSIONAL PROPAGATION—IN CONNECTION WITH THE TEMPERATURE RISE IN FLOWING MEDIUM UPSTREAM FROM HEATING SECTION

RYOZO ECHIGO, SHU HASEGAWA and KOICHI KAMIUTO
Department of Nuclear Engineering, Faculty of Engineering, Kyushu University
Hakozaki, Fukuoka 812, Japan

(*Received* 20 *September* 1974)

Abstract—This paper presents an analytical procedure for simultaneous convective and radiative heat transfer with a fully developed laminar flow in a pipe by taking account of the two-dimensional propagation of radiative transfer and also shows the numerical results on the temperature profiles and the heat-transfer characteristics. In order to solve the energy equation with two-dimensional radiative transfer, one has to solve the entire ranges of the temperature field simultaneously both along the radial and flow directions. Besides the heat flux by thermal radiation emitted from the heating wall propagates upstream so that it is necessary to examine the temperature profiles of the flowing medium to a certain distance upstream from the entrance of the heating section. In this way in order to attempt to solve the governing equation numerically by a finite difference method the dimension of matrix becomes extremely large provided that a satisfactory validity of numerical calculation is required. Consequently the band matrix method is used and the temperature profiles of the medium in the both regions upstream and downstream from the entrance of the heating section are illustrated and the heat-transfer results are discussed in some detail by comparing with those of the one-dimensional transfer of radiation.

NOMENCLATURE

$B(T)$, intensity of black body radiation, $= (\sigma/\pi)T^4$;
c_p, specific heat of fluid at constant pressure;
$FI(\tau_0)$, integral defined by equation (25);
$F_\xi(\tau_x, \tau_0)$, integral defined by equation (24);
f_g, extinction function of thermal radiation from fluid;
f_w, extinction function of thermal radiation from wall;
$H(\tau_0\eta)$, integral defined by equation (14);
$H_\xi(\tau_x, \tau_0\eta)$, integral defined by equation (15);
h_x, local heat-transfer coefficient;
$I_n(y)$, modified Bessel function of first kind with nth order;
i, lattice point of finite difference along axial direction;
j, lattice point of finite difference along radial direction;
$J(T_w)$, radiation intensity from wall;
$K_n(y)$, modified Bessel function of second kind with nth order;
k, thermal conductivity of fluid;
l_0, number of divisions of lattices along axial direction in the region upstream;
l_1, number of divisions of lattices along axial direction in the region downstream;
m, number of divisions of lattices along radial direction;
N_R, dimensionless parameter denoting relative role of conduction to radiation, $= \kappa k/4\sigma T_w^3$;
$Nu_{\xi C}$, local Nusselt number by convection;
$Nu_{\xi R}$, local Nusselt number by radiation;
$Nu_{\xi T}$, local Nusselt number;
n, number of divisions of lattices along circumferential direction;
Pr, Prandtl number;
q_C, convective heat flux;
$\mathbf{q}_R$, radiative heat flux vector;
q_r, radiative heat flux;
q_{Rr}, radial component of radiative heat flux vector;
q_{Rx}, axial component of radiative heat flux vector;
R, pipe radius;
Re, Reynolds number;
r, radial coordinate;
s, distance between medium under consideration and medium situated at another point (Fig. 1);
s_w, distance between medium and wall surface (Fig. 1);
T, temperature of fluid;
T_m, cup-mixing mean temperature of fluid;
T_w, wall temperature;
T_{w0}, wall temperature in the region upstream from heating section;
T_{w1}, wall temperature in the region downstream from heating section;
t, optical distance defined by $(\tau_{x1} - \tau_x\phi)$ (Fig. 1);
U, dimensionless axial velocity, $= u/u_m$;
u, axial velocity of fluid;

u_m, mean axial velocity of fluid;
x, axial coordinate;
x_1, axial coordinate of other medium;
y, independent variable in equation (14);
z_0, optical distance shown in Fig. 1;
z_1, optical distance shown in Fig. 1.

Greek symbols

ε_w, surface emissivity of wall;
η, dimensionless radial coordinate, $= r/R$;
$\Delta\eta$, finite difference of η;
θ, dimensionless temperature of fluid;
θ_m, dimensionless mixing mean temperature of fluid;
θ_{w0}, dimensionless wall temperature in the region upstream;
θ_{w1}, dimensionless wall temperature in the region downstream;
κ, absorption coefficient of fluid for radiation;
μ, viscosity of fluid;
ν, kinematic viscosity of fluid;
ξ, dimensionless axial coordinate, $= (x/R)/(RePr)$;
$\Delta\xi$, finite difference of ξ;
ρ, density of fluid;
σ, Stefan–Boltzman's constant;
τ, optical thickness;
τ_o, optical radius, $= \kappa R$;
τ_s, optical distance between medium under consideration and medium situated at another point (Fig. 1);
τ_{sw}, optical distance between medium and wall surface (Fig. 1);
τ_x, optical axial coordinate, $= \kappa x$;
τ_{x1}, optical axial coordinate, $= \kappa x_1$;
ϕ, azimuthal angle;
$\Delta\phi$, interval of finite difference along circumferential direction.

1. INTRODUCTION

ALTHOUGH a number of studies on composite heat transfer with flowing radiative gases in a circular tube have been performed, further investigations on the heat transfer with the thermal radiation under high temperature and high heat flux have become increasingly important in recent years with the development of high temperature techniques. In general, the radiative heat transfer is characterized by its fundamental nature as having an action-at-a-distance and selection rule for the frequencies, i.e. nongray behavior. Being cumbersome to analyze by taking account of the nongray characteristics of radiating media, there exists, however, no essential difficulty in mathematical treatments and recently a few analytical methods [1–2] have been reported. On the other hand, the action-at-a-distance can be expressed by the integral terms in an energy equation, which results in the integro-differential equation with high order nonlinearity. The analytical treatments on this integro-differential equation have been developed by many researchers and the relevant exposition on the numerical analyses is found in the literature [3–4]. With a few exceptions the radiative heat flux, appeared in the energy equation, is approximately expressed as one-dimensional propagation. In the current study, the propagation of thermal radiation is treated as being two-dimensional and then the contributions of radiative energy from the wall surface and the flowing medium are estimated more exactly and the validity of the one-dimensional analysis of radiation, the temperature profile in the region upstream from an entrance ($x \leqslant 0$), the temperature profile around the starting point of the heating section and the heat-transfer characteristics will be discussed in some detail. Although there are a few reports [5–6] in which the radiative heat transfer is taken into account as being two-dimensional, they are in want of the precision due to the constraints in numerical procedure and the analytical methods used are in want of generality and further the propagation of thermal radiation into the region upstream is not considered at all. Alternatively on account of the axial heat conduction the heat transfer into the region upstream from the region downstream should be considered both for a flow with extremely low velocity [7] even if the effect of radiation is not prominent and for low Prandtl number medium such as liquid metal.

2. THEORETICAL ANALYSIS

2.1. *Descriptions of problem*

The coordinate system and the physical model are illustrated in Fig. 1. The basic assumptions and the postulations introduced for the analysis are as follows.

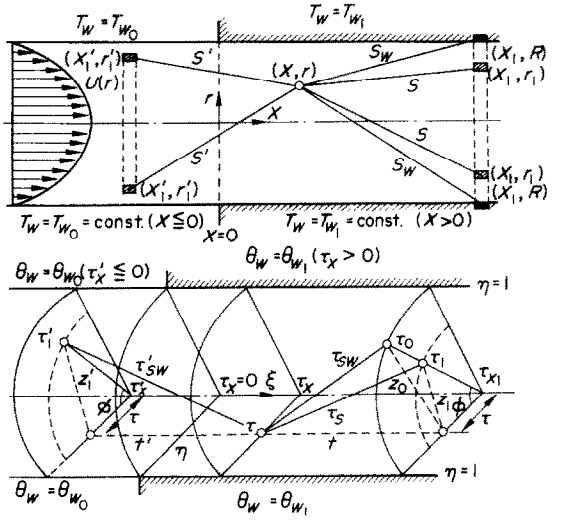

FIG. 1. Coordinate system and physical model.

(i) The flowing medium is a nonscattering radiative gray gas which can absorb and emit thermal radiation.
(ii) The flowing medium is incompressible and the physical properties of the medium are constant.
(iii) The surface of a pipe is a gray diffuse emitter and reflector.

(iv) The flow field is fully developed laminar and its velocity profile is parabolic from the pipe inlet.
(v) The surface temperature is T_{w0} in the region upstream from the heating section ($x \leqslant 0$), and T_{w1} in the region downstream from the heating section ($x > 0$).
(vi) The radiation field is in local radiative equilibrium and the two-dimensional propagation of radiation is taken into account (i.e. the approximation $\partial q_{Rx}/\partial x \ll (1/r)\partial(rq_{Rr})/\partial r$ is not valid).

The formulation of the energy equation with the one-dimensional radiative transfer yields a contradiction to the assumption (v) and the tractable speculation shows that the radiative heat flux from the wall around the entrance region ($x = 0$) may be overestimated by a factor of $2T_{w1}^4/(T_{w0}^4 + T_{w1}^4)$ and, further, a rate of temperature rise along ξ is not evaluated rigorously. In the one-dimensional approximation of radiative transfer the contribution of radiation from the high temperature surface and the heated flowing medium to the medium in the region upstream are not considered at all. Though the foregoing contributions of radiation may be seemingly counterbalanced by each other as the resultant heat-transfer characteristics, it may be stressed that the two-dimensional transfer of radiation has to be taken into account for the purpose of examining the temperature profiles and the heat-transfer mechanism in detail. Further it is worth noting that the consideration of medium upstream from the entrance as a consecutive flowing medium to the heating section is of importance as a basic kind of heat-transfer problem.

2.2. *Basic equations*

Based on the assumption that the flow field is the fully developed laminar flow, the heat balance in the pipe flow yields the basic equation governing the temperature field.

$$\rho c_p u \frac{\partial T}{\partial x} = k \frac{1}{r}\frac{\partial}{\partial r}\left(r\frac{\partial T}{\partial r}\right) - \operatorname{div} \mathbf{q}_R \tag{1}$$

Where $\operatorname{div} \mathbf{q}_R$ is the divergence of the radiative heat flux vector and is given as follows.

$$-\operatorname{div} \mathbf{q}_R = \kappa \int_S J(x_1) f_w(x, r; x_1, R)\,\mathrm{d}S + \kappa \int_V B(x_1, r_1) f_g(x, r; x_1, r_1)\,\mathrm{d}V - 4\kappa B(x, r). \tag{2}$$

In equation (2) the first and second terms on the righthand side represent the contributions by emission from the wall and other flowing medium, respectively and the third term represents self-emission by ϕ medium itself. The boundary conditions are taken as follows.

$$r = 0: \quad \partial T/\partial r = 0$$
$$r = R: \quad T = T_{w1}(x > 0), \quad T = T_{w0}(x \leqslant 0). \tag{3}$$
$$x = -\infty: \quad T = T_{w0}. \tag{4}$$

Since equation (4) in the boundary conditions has to be treated carefully in numerical calculations, it will be discussed later. Referring to Fig. 1, equation (2) becomes

$$-\operatorname{div} \mathbf{q}_R = 2\kappa \frac{\sigma}{\pi} \int_{-\infty}^{\infty} \int_0^{\pi} T_w^4(x_1) \frac{\exp(-\kappa s_w)}{s_w^3} \times R(R - r.\cos\phi)\,\mathrm{d}\phi\,\mathrm{d}x_1 + 2\kappa \frac{2\sigma}{\pi} \times \int_0^R r_1 \int_{-\infty}^{\infty} T^4(x_1, r_1) \left\{ \int_0^{\pi} \frac{\exp(-\kappa s)}{s^2}\,\mathrm{d}\phi \right\} \times \mathrm{d}x_1\,\mathrm{d}r_1 - 4\kappa\sigma T^4(x, r). \tag{5}$$

Multiplying both sides of equation (1) by (R^2/kT_{w1}) and arranging it in the dimensionless form, the energy equation can be manipulated into the form,

$$\tfrac{1}{2}U\frac{\partial\theta}{\partial\xi} = \frac{1}{\eta}\frac{\partial}{\partial\eta}\left(\eta\frac{\partial\theta}{\partial\eta}\right) + \frac{\tau_0^3}{2N_R}\int_{-\infty}^{\infty} \theta_w^4(\tau_{x1}) \times \left\{\frac{1}{\pi}\int_0^{\pi} \frac{\exp(-\tau_{sw})}{\tau_{sw}^3}(\tau_0 - \tau\cos\phi)\,\mathrm{d}\phi\right\}\mathrm{d}\tau_{x1} + \frac{\tau_0^4}{2N_R}\int_0^1 \eta_1 \int_{-\infty}^{\infty} \theta^4(\tau_{x1}, \eta_1) \times \left\{\frac{1}{\pi}\int_0^{\pi} \frac{\exp(-\tau_s)}{\tau_s^2}\,\mathrm{d}\phi\right\}\mathrm{d}\tau_{x1}\,\mathrm{d}\eta_1 - \frac{\tau_0^2}{N_R}\theta^4(\tau_x, \eta) \tag{6}$$

where the dimensionless variables and parameters in equation (6) are defined as

$$\theta = T/T_w, \quad \xi = (x/R)/RePr, \quad Re = 2u_m R/\nu,$$
$$Pr = c_p\mu/k, \quad N_R = k\kappa/4\sigma T_{w1}^3, \quad \tau_0 = \kappa R,$$
$$\tau = \kappa r, \quad \tau_x = \kappa x, \quad \tau_{sw} = \kappa s_w, \quad \tau_s = \kappa s,$$
$$\eta = r/R = \tau/\tau_0, \quad U = u/u_m = 2(1-\eta^2). \tag{7}$$

Referring to Fig. 1 again τ_{sw} and τ_s are given by

$$\tau_{sw} = (t^2 + z_0^2)^{\frac{1}{2}} = [(\tau_x - \tau_{x1})^2 + \tau^2 + \tau_0^2 - 2\tau\tau_0\cos\phi]^{\frac{1}{2}} \tag{8}$$
$$\tau_s = (t^2 + z_1^2)^{\frac{1}{2}} = [(\tau_x - \tau_{x1})^2 + \tau^2 + \tau_1^2 - 2\tau\tau_1\cos\phi]^{\frac{1}{2}}. \tag{9}$$

The boundary conditions are rewritten as follows.

$$\eta = 0: \quad \partial\theta/\partial\eta = 0, \qquad \eta = 1: \quad \theta = \theta_w \tag{10}$$
$$\xi = -\infty: \quad \theta = \theta_{w0} \tag{11}$$

where θ_w denotes the dimensionless wall temperature and is given by,

$$\theta_w = \begin{cases} \theta_{w1}(= 1{\cdot}0) & \tau_x > 0 (x > 0) \\ \theta_{w0} & \tau_x \leqslant 0 (x \leqslant 0). \end{cases} \tag{12}$$

2.3. *Simplification of radiative heat flux*

Performing the integration on τ_{x_1} under consideration of $\tau_{x_1} - \tau_x = t$ and $\mathrm{d}\tau_{x_1} = \mathrm{d}t$ in the radiative term which denotes the contribution of radiation from the

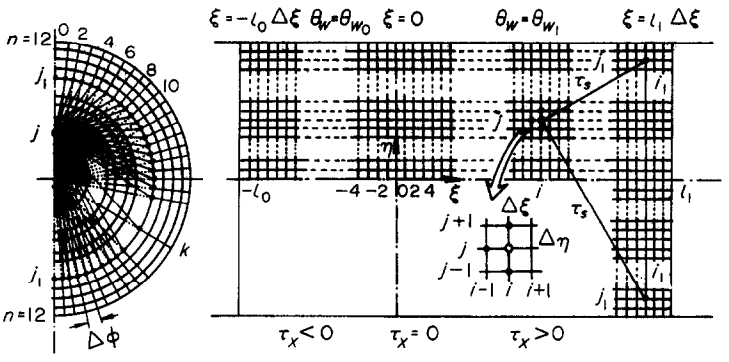

FIG. 2. Lattice of finite difference.

wall, the radiative term becomes as follows irrespective of the signs of τ_x.

$$\frac{1}{\pi}\int_{-\infty}^{\infty}\theta_w^4(\tau_{x_1})\left\{\int_0^{\pi}\frac{\exp(-\tau_{sw})}{\tau_{sw}^3}(\tau_o-\tau\cos\phi)\,d\phi\right\}d\tau_{x_1}$$
$$=\frac{1}{\pi}(\theta_{w_1}^4+\theta_{w_0}^4)\int_0^{\infty}\int_0^{\pi}\frac{\exp(-\tau_{sw})}{\tau_{sw}^3}(\tau_o-\tau\cos\phi)\,d\phi\,dt$$
$$+\frac{1}{\pi}(\theta_{w_1}^4-\theta_{w_0}^4)\int_0^{\tau_x}\int_0^{\pi}\frac{\exp(-\tau_{sw})}{\tau_{sw}^3}(\tau_o-\tau\cos\phi)\,d\phi\,dt$$
$$=(\theta_{w_1}^4+\theta_{w_0}^4)H(\tau_o\eta)+(\theta_{w_1}^4-\theta_{w_0}^4)H_\xi(\tau_x,\tau_o\eta) \qquad (13)$$

where $H(\tau_o\eta)$ is the same function as the extinction function of radiation from the wall used in the one-dimensional approximation of radiative transfer and is defined as

$$H(\tau_o\eta)=\int_1^{\infty}K_1(\tau_o\eta)I_o(\tau_o\eta y)y^{-1}\,dy \qquad (14)$$

and $H_\xi(\tau_x,\tau_o\eta)$ is defined as follows.

$$H_\xi(\tau_x,\tau_o\eta)=\frac{1}{\pi}\int_0^{\tau_x}\int_0^{\pi}\frac{\exp(-\tau_{sw})}{\tau_{sw}^3}(\tau_o-\tau\cos\phi)\,d\phi\,dt. \qquad (15)$$

Here, $I_n(y)$ and $K_n(y)$ are the modified Bessel functions of the first and second kind with nth order, respectively. The radiative term which denotes the contribution of radiation from other medium cannot be calculated independently because of the presence of unknown temperatures $\theta(\tau_{x_1},\eta_1)$ in the integrant in equation (6).

3. NUMERICAL ANALYSIS

3.1. *Principal procedure*

Energy equation (6) constitutes an integro-differential equation with high order nonlinearity on θ and it seems to be formidable to get an analytical solution. Therefore, one has to calculate numerically and a finite difference method may be a plausible means. It may be pointed out concerning the numerical computation that as the progressive procedure on ξ cannot be applied to solve the energy equation, the problems should be solved simultaneously in a proper controlled volume and that the number of the grids of finite difference in the controlled volume is restricted to the capacity of the computer. The controlled volume must include not only the region upstream ($\xi \leqslant 0$) but the region downstream ($\xi > 0$). Therefore, transforming the energy equation into the algebraic equations by the finite difference method, we have to solve the simultaneous linear equations having an extremely large dimension.

3.2. *Finite difference approximations*

The equally spaced lattices of finite difference are illustrated in Fig. 2. The intervals of finite difference along ξ, η and ϕ are designated $\Delta\xi$, $\Delta\eta$ and $\Delta\phi$, respectively, and the radius is divided into m-equal increments and the circumference into n-equal increments (i.e. $m.\Delta\eta = 1, n\cdot\Delta\phi = \pi$). $\Delta\phi$ is not restricted especially in a magnitude but $\Delta\eta$ is restricted because of the precision in the evaluation of heat-transfer coefficient. η is divided into ten equal increments in executing the computation ($m = 10$, $\Delta\eta = 0{\cdot}1$) and further the lattice intervals near the wall is subdivided into two equal increments so as to elevate the precision in the evaluation of heat-transfer coefficients. The circumference is divided into thirty-six equal intervals ($n = 36, \Delta\phi = \pi/36$) and the integrals on ϕ is estimated by the trapezoidal formula. Intervals of finite difference along ξ will be discussed later in detail. In practice, the numerical calculations cannot be performed in the region from $-\infty$ to $+\infty$ with respect to ξ and therefore the controlled volume should be set in a certain region from $-l_0\Delta\xi$ to $l_1\Delta\xi$ along ξ. As the total number of lattices of finite difference should be determined by the capacity of the computer, and therefore we choose $l_0 = 9$ and $l_1 = 21$. However, the contribution of radiation is considered in the region from $-(l_0+l_1)\Delta\xi$ to $(l_0+l_1)\Delta\xi$ around an arbitrary point ($\xi = i\cdot\Delta\xi$) and further the temperatures in the region outside of the controlled volume are approximated to be identical with those at $\xi = -l_0\Delta\xi$ and $l_1\Delta\xi$ as illustrated in Fig. 3. In such a case it is favorable to satisfy the following condition,

$$\kappa(l_0+l_1)\Delta x = (l_0+l_1)\Delta\xi RePr\tau_o \gg 1 \qquad (16)$$

(this means that the radiation is attenuated sufficiently when it travels for an optical path of $\kappa(l_0+l_1)\Delta x$) and further it is desirable to consider up to 0·1 where the convective temperature field develops sufficiently, provided the radiation is not taken into account.

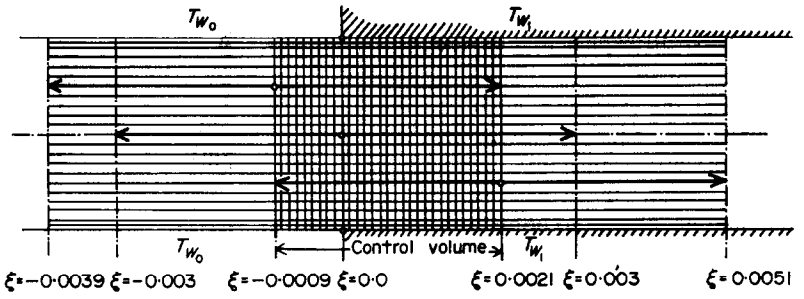

FIG. 3. Floating region for calculating the radiative term.

3.3. *Numerical methods*

By the finite difference approximations the equation (6) results in

$$-\frac{1-(j\cdot\Delta\eta)^2}{\Delta\xi}\theta(i-1,j)-\left(1-\frac{1}{2j}\right)\frac{1}{(\Delta\eta)^2}\theta(i,j-1)+\left\{\frac{1-(j\cdot\Delta\eta)^2}{\Delta\xi}+\frac{2}{(\Delta\eta)^2}\right\}\theta(i,j)-\left(1+\frac{1}{2j}\right)\frac{1}{(\Delta\eta)^2}\theta(i,j+1)$$
$$=\frac{\tau_o^3}{2N_R}\{(\theta_{w_1}^4+\theta_{w_0}^4)H(\tau_o j\Delta\eta)+(\theta_{w_1}^4-\theta_{w_0}^4)H_\xi(\tau_x,\tau_o\eta)\}+\frac{\tau_o^4}{2N_R}\int_0^1\eta_1\int_{-\infty}^{\infty}\theta^4(\tau_{x_1},\eta_1)\times\left\{\frac{1}{\pi}\int_0^{\pi}\frac{\exp(-\tau_s)}{\tau_s^2}\,d\phi\right\}d\tau_{x_1}\,d\eta_1-\frac{\tau_o^2}{N_R}\theta^4(i,j). \quad (17)$$

The integrals of radiative terms on the r.h.s. in equation (17) are calculated by the trapezoidal or Simpson's formula. After the solution $\theta(i,j)^{(0)}$ in the entire region of controlled volume without radiation is obtained, it substitutes the radiative terms to obtain the first approximation $\theta(i,j)^{(1)}$ and then the similar computations are performed repeatedly until the prescribed convergence is satisfied. The convergence criterion is given by the following inequality.

$$|\theta(i,j)^{(p)}-\theta(i,j)^{(p-1)}|<0.0005. \quad (18)$$

It needs to solve simultaneous linear algebraic equations of large dimension in order to get the solution for the entire ranges of x and r. Fortunately the non-zero elements in the coefficient matrix are comparatively few, and then the band matrix method [8] is plausible for the present system.

3.4. *Few remarks on performing numerical calculations*

In order to get a better perspective of the numerical calculations, and the evaluation results, it is worth presenting the following discussions.

(i) At first we speculate the intervals of finite difference along ξ. It is noticed easily that τ_{x1} is used as a variable in the integration with respect to ξ in the radiative term. Designating an infinitesimal of τ_{x1} as $\Delta\tau_{x1}$, there exists a following relation between $\Delta\tau_{x1}$ and an interval of finite difference $\Delta\xi$.

$$\Delta\tau_{x1}=\kappa x=\Delta\xi\cdot Re\cdot Pr\cdot\tau_o. \quad (19)$$

Accordingly, it is found that the precision of numerical integration along ξ does not depend on $\Delta\xi$ but $\tau_o RePr\Delta\xi$. Based on a theory of stability of finite difference scheme on the parabolic partial differential equation, a ratio of $\Delta\eta$ to $\Delta\xi$ is not restricted especially so long as the finite difference technique of an implicit method is used. However, even if the finite difference approximation is performed with the aid of an implicit method, $\Delta\eta/\Delta\xi$ is not arbitrary because $\Delta\tau_{x1}$ is restricted to the precision in the numerical integration of the radiative term. Then $\Delta\xi$ is limited in a magnitude. In order to eliminate this restriction on the precision of numerical integration with respect to ξ, it will be necessary to approximate the integrant by a proper polynomial based on the data in some lattice points and to integrate this polynomial analytically.

(ii) Next a settlement of the starting point of the heating section is discussed briefly. The wall temperature varies stepwisely from T_{w0} to T_{w1} at the starting point of the heating section and it has to be stressed that the fluid temperature at $\xi=0$ is uniform provided thermal radiation is absent. On account of finite differentiation of the controlled volume there exist two types of variation of the wall temperature and they are illustrated schematically in Fig. 4 when the radiative transfer is not taken into consideration. In case of (I) in Fig. 4 the temperature of medium at the starting point of the heating section in the convective temperature field has already been raised because of the grid for finite difference adopted here (shown in Fig. 2) so that the wall temperature between $\xi=-\Delta\xi$ to $\xi=0.0^+$ has to

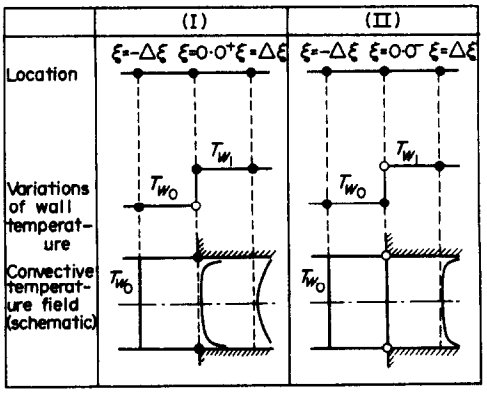

FIG. 4. Variations of wall temperature near the starting point of heating section.

be regarded as T_{w1}, in other words, the starting point of the heating section must be shifted to $\xi = -\Delta\xi$. On the other hand, in case of (II) in Fig. 4 the temperature of medium at the starting point of the heating section is uniform and equals to initial temperature T_{w0}, because the wall temperature at that point is restricted to T_{w0}, so that this is plausible for a settlement of the starting point. Accordingly we adopt case (II) in Fig. 4 as the variation of the wall temperature and the starting point of the heating section is denoted by $\xi = 0{\cdot}0^-$. The starting point of the heating section may be, however, dependent on the type of the grid for finite difference.

(iii) Finally as already shown the convective term in the energy equation is approximated by the following finite difference.

$$\frac{\partial\theta}{\partial x} = \frac{\theta(i,j)-\theta(i-1,j)}{\Delta x}. \tag{20}$$

At first, it is expected that $\partial\theta/\partial x$ could be approximated by the following finite difference approximation.

$$\frac{\partial\theta}{\partial x} = \frac{\theta(i+1,j)-\theta(i-1,j)}{2\Delta x}. \tag{21}$$

With this approximation, however, it was not easy to get a tractable convergence which showed a wavy vibrating profile of temperature along the radius. Consequently the finite difference approximation of $\partial\theta/\partial x$ is performed by equation (20).

4. EVALUATION RESULTS AND DISCUSSIONS

4.1. *Temperature profiles*

The typical results of temperature profiles calculated here are illustrated in Figs. 5–8. Figures 5 and 6 illustrate the variation of the temperature profiles with the parameters of a reciprocal of Graetz number, ξ. The broken lines denote temperature profiles without radiation. Figure 5 corresponds to the results for $\tau_o = 1{\cdot}0$ and $RePr = 1000$. The temperature profiles in the region upstream from the heating section are characterized by the temperature peak near the wall. The reason why there exists the temperature peak near the wall in the region upstream is that the medium in this region is heated by the radiation from the region downstream and, therefore, is effected strongly by the radiation from the heating wall in the region downstream. Since the medium in the region upstream is heated by the radiation alone, a rate of temperature rise is rapidly reduced as aparting from the starting point of the heating section and the temperature in $\xi < -0{\cdot}0005$ is almost as same as inlet temperature, T_{w0}. Chained lines in the central part of a pipe in the region downstream are obtained by the actual calculations, which may be attributed to the presence of a singular point on the central axis of a pipe and such a behavior is also observed in the one-dimensional analysis of radiation. However, as these curves do not satisfy the boundary condition, i.e. $\partial\theta/\partial r = 0$ at $r = 0$, the physically plausible curves are drawn by the solid

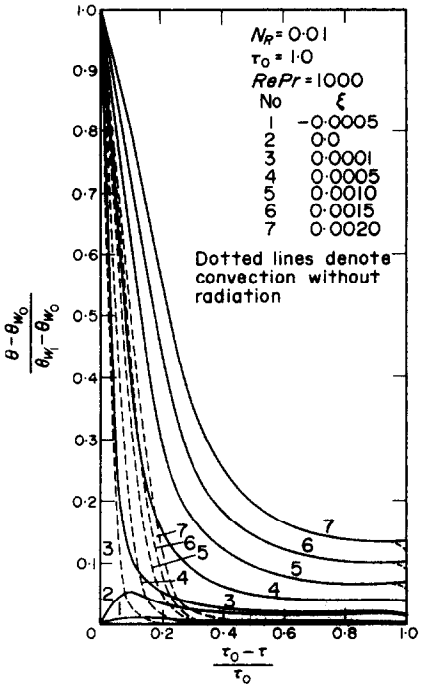

FIG. 5. Temperature profiles vs $(\tau_o-\tau)/\tau_o$ (effect of ξ). $N_R = 0{\cdot}01$; $\tau_o = 1{\cdot}0$; $RePr = 1000$.

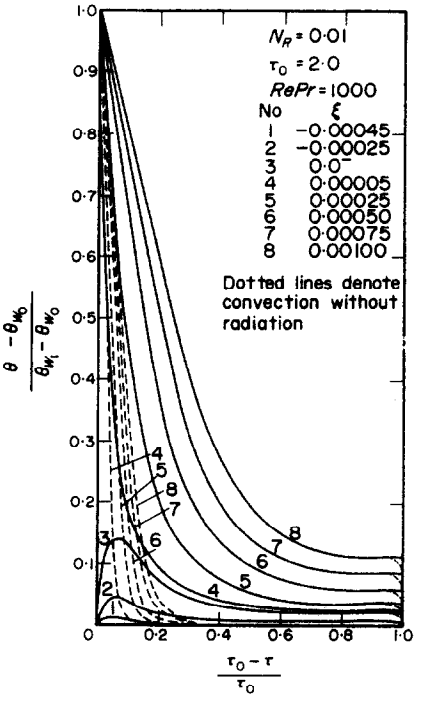

FIG. 6. Temperature profiles vs $(\tau_o-\tau)/\tau_o$ (effect of ξ). $N_R = 0{\cdot}01$; $\tau_o = 2{\cdot}0$; $RePr = 1000$.

lines in this and subsequent figures. Figure 6 illustrates the temperature profiles for $\tau_o = 2{\cdot}0$, $N_R = 0{\cdot}01$ and $RePr = 1000$ with the variation of parameter, ξ. The effects of N_R on the temperature profiles are shown in Fig. 7. For the medium upstream, i.e. for $\xi \leqslant 0{\cdot}0^-$, the temperature rises uniformly in the entire region of a pipe as N_R decreases. On the contrary, as N_R increases and is larger than 0·1, the temperature rise

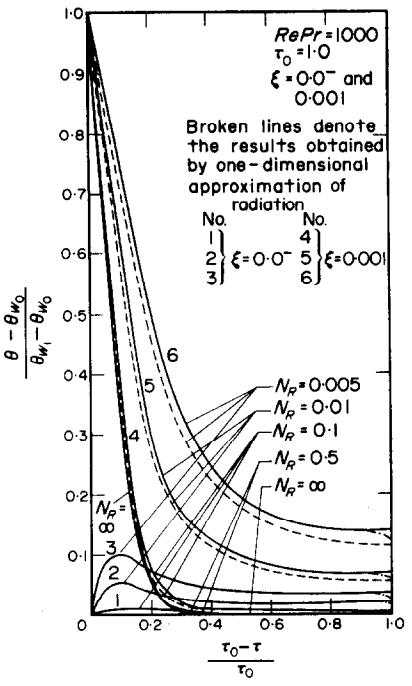

FIG. 7. Temperature profiles vs $(\tau_o-\tau)/\tau_o$ (effect of N_R). $RePr = 1000$; $\tau_o = 1{\cdot}0$; $\xi = 0{\cdot}0^-$ and 0·001. Broken lines denote the results obtained by one-dimensional approximation of radiation. 1, 2, 3, $\xi = 0{\cdot}0^-$: 4, 5, 6, $\xi = 0{\cdot}001$.

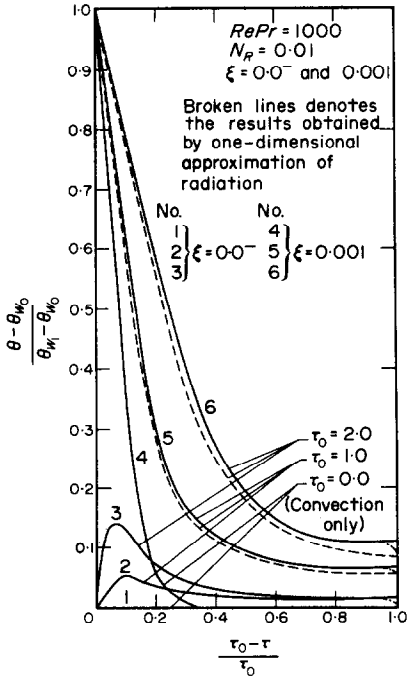

FIG. 8. Temperature profiles vs $(\tau_o-\tau)/\tau_o$ (effect of τ_o). $RePr = 1000$; $N_R = 0{\cdot}01$. Broken lines denote the results obtained by one-dimensional approximation of radiation. 1, 2, 3, $\xi = 0{\cdot}0^-$; 4, 5, 6, $\xi = 0{\cdot}001$.

in the region upstream almost diminishes and approaches to the case of the one-dimensional approximation of radiation. For the medium downstream, corresponding to $\xi = 0{\cdot}001$, the temperature profiles are not distinguished from that without radiation as N_R is larger than 0·1. The temperature profiles obtained by the one-dimensional analysis of radiation are lower than those obtained by the two-dimensional one and further the temperature difference between them tends to increase as N_R decreases. The influences of the optical thickness τ_o are depicted in Fig. 8 for $RePr = 1000$ and $N_R = 0{\cdot}01$. In the region upstream, as τ_o increases, the temperature peak near the wall becomes higher and approaches to the close vicinity of the wall. The temperature in the central part is not elevated even if τ_o increases. Such phenomena may be attributed to the fact that the radiation energy penetrates into the medium in case of small τ_o, while in case of large τ_o the radiation energy can not travel into the deep central core even if the wall is kept at high temperature and emits radiation intensively. In the region downstream the remarkable temperature rise is observed in the vicinity of the wall, while the temperature in the central core is rather lower. Compared with the temperature profiles obtained by the one-dimensional analysis of radiation and those obtained by the two-dimensional one for constant τ_o, the former is lower than the latter. As to an effect of $RePr$ on the temperature profile in the region upstream the temperature peak near the wall is higher with decreasing $RePr$ but the temperature in the central part is elevated with increasing $RePr$. In general, as the residence time of medium in a pipe is longer with decreasing $RePr$ and then the medium absorbs much radiation with the increment of residence time and the radiation from the region downstream penetrates easily into the region upstream with a decrease of $RePr$, the temperature rise in a pipe ought to be higher with a decrease of $RePr$ for constant N_R and τ_o.

4.2. *Cup-mixing mean temperatures*

The cup-mixing mean temperature in a dimensionless form is defined as

$$\theta_m = \int_0^1 U(\eta)\theta(\eta)\eta\,d\eta \Big/ \int_0^1 U(\eta)\eta\,d\eta. \qquad (22)$$

Figure 9 illustrates the relation between θ_m and ξ as the parameters of denoting the relative role of conduction to radiation N_R and the optical thickness τ_o. In case of constant $RePr$ and τ_o, the radiation emitted from the medium in the region downstream penetrates into the deeper region upstream as N_R decreases, so that θ_m increases appreciably through the wide region upstream. In case of constant $RePr$ and N_R, the larger τ_o is, the higher θ_m is, but θ_m decreases rapidly as aparting from the entrance of the heating section. Compared to the results obtained by the one-dimensional analysis of radiation with those obtained by the two-dimensional one in the region downstream, it is found that θ_m is underestimated in case of the one-dimensional analysis. Reference to the figure reveals the fact that although the radiation from the wall surface in the region upstream is overestimated near the starting point of the heating section in the one-dimensional analysis, the temperature rise in the

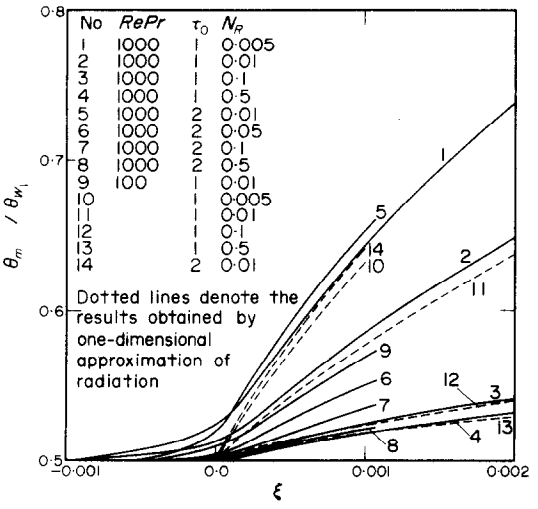

FIG. 9. Cup-mixing mean temperature vs ξ

region upstream is ignored completely. By the way, although, in the current study, the contribution of radiation from other medium is underestimated due to the limited controlled volume, θ_m obtained by the two-dimensional analysis of radiative transfer is rather higher than that obtained by the one-dimensional one. Therefore these results are considered to be evaluated in perspective of appropriate controlled volume and the substantial difference will not be found even if the computations will be repeated more exactly by taking the larger controlled volume into account. The detailed examination on this figure shows that when N_R becomes large and radiation is not dominant, there exists a region where the temperature profiles obtained by the one-dimensional approximation are higher than those obtained by the two-dimensional propagation of radiation. This is understood as follows. Since the temperature rise in the region upstream is small for large N_R in case of the two-dimensional analysis and such a situation resembles the assumption used by the one-dimensional case in which the contribution of radiation from the wall surface in the region upstream is overestimated, θ_m obtained by the one-dimensional approximation is higher than that obtained by the two-dimensional treatment. In the region far downstream θ_m obtained by the two-dimensional analysis, however, is higher than that obtained by the one-dimensional one even if N_R is large. This fact indicates that the contribution of radiation from other medium is underestimated by the one-dimensional approximation in this region. The examination on the variation of θ_m with the variation of parameter $RePr$ is not reproduced here on account of a similar trend as discussed in Section 4.1.

4.3. *Net radiative heat flux at wall surface*

The net radiative heat flux at the wall surface q_r consists of leaving and incoming fluxes of radiation and is obtained by subtracting the radiation heat flux which is emitted by the other wall and reaches to the controlled surface after being attenuated by the flowing medium and the radiative heat flux emitted by the flowing medium of the entire controlled volume from the radiative heat flux emitted by the controlled surface.

$$q_r = \frac{kT_{w1}}{R}\left[\frac{\tau_o}{4N_R}\theta_w^4 - \frac{\tau_o^4}{2N_R}\right.$$
$$\times\{(\theta_{w1}^4+\theta_{w0}^4)FI(\tau_o)+(\theta_{w1}^4-\theta_{w0}^4)F_\xi(\tau_x,\tau_o)\}$$
$$-\frac{\tau_o^4}{2N_R}\int_{-\infty}^{\infty}\int_0^1\theta^4(\tau_{x1},\eta_1)\left\{\frac{1}{\pi}\int_0^\pi\frac{\exp(-\tau_s)}{\tau_s^3}\right.$$
$$\left.\left.\times(1-\eta_1\cos\phi)\,d\phi\right\}\eta_1\,d\eta_1\,d\tau_{x1}\right] \quad (23)$$

where

$$F_\xi(\tau_x,\tau_0)=\int_0^{\tau_x}\frac{1}{\pi}\int_0^\pi\frac{\exp(-\tau_{sw})}{\tau_{sw}^4}(1-\cos\phi)^2\,d\phi\,dt \quad (24)$$

$$FI(\tau_o)=\int_0^\infty\frac{1}{\pi}\int_0^\pi\frac{\exp(-\tau_{sw})}{\tau_{sw}^4}(1-\cos\phi)^2\,d\phi\,dt \quad (25)$$

here $FI = 0{\cdot}297977$ for $\tau_o = 0{\cdot}5$, $FI = 0{\cdot}203573$ for $\tau_o = 1{\cdot}0$ and $FI = 0{\cdot}118225$ for $\tau_o = 2{\cdot}0$. In case of $\theta_{w0} = \theta_{w1}$, q_r in equation (23) is agreed with that obtained by the one-dimensional approximation of radiative heat flux. Figure 10 illustrates the relation of q_r vs ξ. In the domain of $\xi \leqslant 0$ the radiative heat flux is negative and the absolute value is plotted in the figure. The radiative heat flux is sufficiently decayed in the controlled volume in the region upstream and for constant N_R as τ_o becomes large, the trend of drastic extinction of the radiative heat flux is found. This fact

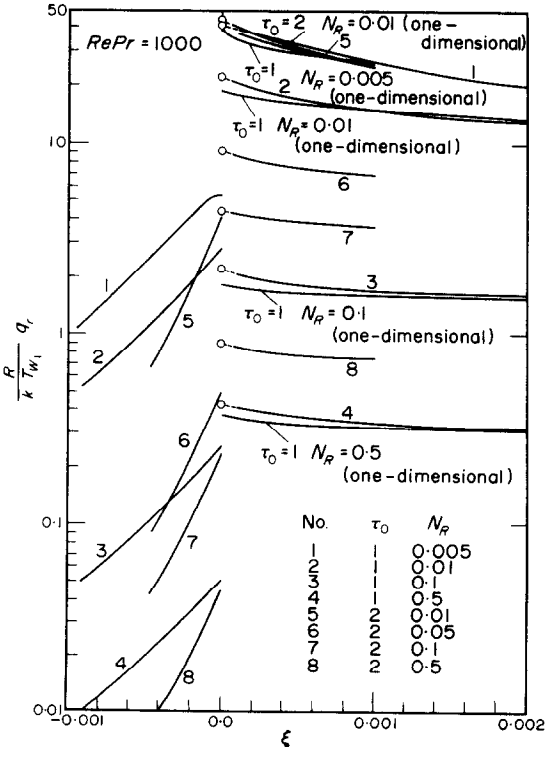

FIG. 10. Net radiative heat flux at the wall vs ξ (in case of $RePr = 1000$, in $\xi \leqslant 0$ radiative heat fluxes are negative but in this figure the absolute values are illustrated).

seems to show the controlled volume adopted here in the region upstream is valid. In the region downstream, the radiative heat flux is increased as the parameter N_R decreases for constant optical thickness τ_o, while the radiative heat flux is shown to decrease as the optical thickness τ_o decreases when the parameter N_R is held constant. Further it is found that the radiative heat flux obtained by the one-dimensional approximation of radiation is smaller than that obtained by the two-dimensional estimation near the starting point of the heating section. This is due to the fact that in the region downstream the radiative heat flux by the one-dimensional analysis is smaller than that by the two-dimensional one because of the underestimation of radiation from the wall surface in the region upstream, provided that the contribution of radiation from other medium is not underestimated. But, for small N_R the radiative heat flux by the one-dimensional analysis tends to be larger than that by the two-dimensional one. This is caused by the fact that the contribution of radiation from other medium calculated by the one-dimensional analysis is underestimated than that calculated by the two-dimensional one.

4.4. *Heat-transfer characteristics*

Nusselt number is defined so as to evaluate the heat-transfer characteristics and for the two-dimensional propagation of radiation the local Nusselt numbers are defined in a similar way to the one-dimensional radiative transfer.

$$Nu_{\xi T} = \frac{h_x . 2R}{k} = \frac{q_C + q_R}{k(T_w - T_m)} . 2R = Nu_{\xi C} + Nu_{\xi R} \quad (26)$$

$$Nu_{\xi C} = 2\left(\frac{\partial\theta}{\partial\eta}\right)_{\eta=1} / (\theta_w - \theta_m) \quad (27)$$

$$Nu_{\xi R} = 2\left(\frac{kT_{w1}}{R}\right) q_R / (\theta_w - \theta_m). \quad (28)$$

Figure 11 illustrates the relation between these local Nusselt numbers against ξ. Reference to Fig. 11 for $RePr = 1000$ and $\tau_o = 1{\cdot}0$ reveals that $Nu_{\xi T}$ is increasing rapidly far from the starting point of the heating section upstream. It is found that the heat-transfer characteristics obtained by the one-dimensional analysis are underestimated than those obtained by the two-dimensional one near the starting point of the heating section down the stream. This is due to such a trend that $Nu_{\xi C}$ and $Nu_{\xi R}$ in the one-dimensional case is larger than those in the two-dimensional one. The broken lines in these figures, denoted by $Nu_{\xi C}$, tend to be small as N_R decreases and such a phenomenon indicates that a ratio of convective heat transfer to the overall heat transfer decreases with a decrease of N_R. Reference to Fig. 11 again for $RePr = 1000$ and $\tau_o = 2{\cdot}0$ shows that the results obtained by the one-dimensional approximation, being depicted only for $N_R = 0{\cdot}01$, are smaller than that obtained by the two-dimensional evaluation.

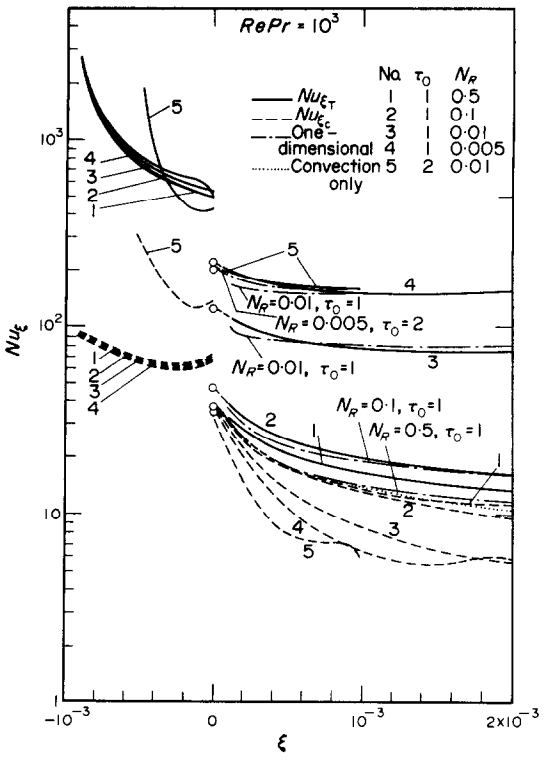

FIG. 11. Local Nusselt number $Nu_{\xi T}$ and $Nu_{\xi C}$ vs ξ ($RePr = 1000$).

5. CONCLUDING REMARKS

On composite heat transfer of laminar flow in a circular tube the energy equation with the two-dimensional propagation of thermal radiation is solved numerically for a certain controlled volume involving the region upstream from the starting point of the heating section. Further the validity of one-dimensional propagation of radiation, the temperature profiles around the entrance of the heating section and the heat-transfer characteristics have been examined in some detail. The important conclusions obtained here are as follows:

(1) For large dimensionless parameter N_R the temperatures in the region upstream do not increase and are almost identical to those in case of pure convection. For small N_R the temperature profiles in the region upstream are characterized by the temperature peak near the wall, which becomes higher with a decrease of N_R and approaches to the close vicinity of wall with an increase of optical thickness, τ_o. In general, for constant τ_o the temperature rise in the region upstream becomes prominent with a decrease of N_R and the temperature is elevated to a certain extent up to the region far upstream and for constant N_R a rate of temperature rise decreases with an increase of τ_o.

(2) The temperature profiles and the mixed mean temperatures obtained by the one-dimensional approximation of radiation tend to be lower than those obtained by the two-dimensional evaluation of radiation at small reciprocal of Graetz number ξ and such a tendency is emphasized for small N_R and for large τ_o.

(3) The local Nusselt number, $Nu_{\xi T}$ in the region upstream from the heating section increases rapidly as aparting from the starting point of the heating section. The heat-transfer characteristics obtained by the one-dimensional analysis is underestimated than those obtained by the two-dimensional one near the entrance of the heating section in the region downstream.

Acknowledgements—The authors wish to express their gratitude to Prof. Y. Katto, University of Tokyo, who stimulated the authors to perform this study and also to acknowledge the financial support by the Ministry of Education from the research grant for fiscal year of 1972 (No. 758048 for general research, type C). These calculations are performed with the aid of FACOM 230-60 at Computer Center, Kyushu University.

REFERENCES

1. R. Echigo, S. Hasegawa and Y. Miyazaki, Composite heat transfer with thermal radiation in non-gray medium. Part 1: Interaction of radiation with conduction, *Int. J. Heat Mass Transfer* **14**, 2001 (1971).
2. R. D. Cess, P. Mighdoll and S. M. Tiwari, Infrared radiative heat transfer in non-gray medium, *Int. J. Heat Mass Transfer* **10**, 1921 (1967).
3. R. Viskanta, Interaction of heat transfer by conduction, convection, and radiation in a radiating fluid, *J. Heat Transfer* **85C**, 318 (1963).
4. Y. Kurosaki, Heat transfer by radiation and other transport mechanisms (2nd Report, flow between parallel flat plates with simultaneous radiation and convection), *Proc. Japan Soc. Mech. Engrs* **35**(278), 2099 (1969).
5. T. H. Einstein, Radiant heat transfer to absorbing gases enclosed in a circular pipe with conduction, gas flow, and internal heat generation, NASA TR R-156 (1963).
6. S. Desoto, Coupled radiation, conduction and convection in entrance region flow, *Int. J. Heat Mass Transfer* **11**, 39 (1968).
7. F. H. Verhoff and D. P. Fisher, A numerical solution of the Graetz problem with axial conduction included, *J. Heat Transfer* **95C**, 132 (1973).
8. N. Yoshimura, Y. Nobuhara and R. Sakurai, *Series on Structure Engineering with Computer*, II-2-B, (in Japanese). Baifukan, Tokyo (1972).

TRANSFERT DE CHALEUR MIXTE DANS UN TUBE AVEC RAYONNEMENT THERMIQUE BIDIMENSIONNEL—EN RELATION AVEC L'AUGMENTATION DE TEMPERATURE DANS L'ECOULEMENT EN AMONT DE LA SECTION DE CHAUFFAGE

Résumé—L'article présente une méthode analytique pour l'étude du transfert de chaleur par convection et rayonnement simultanés en écoulement laminaire établi dans un tube en tenant compte de la propagation bidimensionnelle du rayonnement. Sont également présentés les résultats numériques relatifs aux profils de température et aux caractéristiques du transfert thermique. Afin de résoudre l'équation de l'énergie avec rayonnement thermique bidimensionnel, l'on doit traiter simultanément, toute l'étendue du champ de température à la fois dans la direction radiale et dans la direction de l'écoulement. De plus, le flux de chaleur par rayonnement thermique émis par les parois chauffantes se propage à l'amont, si bien qu'il est nécessaire d'examiner les profils de température dans l'écoulement à partir d'une certaine distance située à l'amont de l'entrée de la section de chauffage. Ainsi, afin de tenter de résoudre l'équation fondamentale numériquement à l'aide d'une méthode de différences finies, la dimension de la matrice devient très grande pour que la validité exigée des calculs numériques soit satisfaisante. En conséquence, la méthode de zone est utilisée et les profils de température dans le fluide sont calculés aux niveaux amont et aval de la région d'entrée de la section de chauffage. Les résultats de transfert de chaleur sont discutés en détail par comparaison avec ceux du transfert par rayonnement unidimensionnel.

WÄRMEÜBERGANG IM ROHR BEI ZWEIDIMENSIONALER WÄRMESTRAHLUNG IN VERBINDUNG MIT DEM TEMPERATURANSTIEG IN DER STRÖMUNG STROMAUFWÄRTS VOM BEHEIZTEN ABSCHNITT

Zusammenfassung—Der Aufsatz stellt die Analyse des gleichzeitigen Wärmeaustausches durch Konvektion und zweidimensionale Strahlung bei ausgebildeter laminarer Rohrströmung vor. Für die Temperaturprofile und den Wärmeübergang werden Zahlenergebnisse mitgeteilt. Die Lösung der Energiegleichung erfolgt unter Berücksichtigung der zweidimensionalen Wärmestrahlung nach Ermittlung des Temperaturverlaufs in Strömungsrichtung und quer zur Strömung. Durch Abstrahlung der Heizfläche findet Wärmeaustausch bereits stromaufwärts statt, so daß es erforderlich ist, die Temperaturprofile in der Strömung in einiger Entfernung vor dem beheizten Abschnitt zu überprüfen. Auf diese Weise erhält man bei Anwendung der Methode der finiten Differenzen zur Lösung der Ausgangsgleichung eine Lösungsmatrix von erheblichem Umfang, wenn die numerische Auswertung befriedigende Genauigkeit ergeben soll. Folglich wird von der Band-Matrix-Methode Gebrauch gemacht, und die Temperaturprofile werden stromaufwärts und stromabwärts vom Eintritt in die Heizstrecke erstellt. Die Ergebnisse für den Wärmeübergang werden im Vergleich mit dem Wärmeaustausch bei eindimensionaler Wärmestrahlung zur Diskussion gestellt.

СЛОЖНЫЙ ТЕПЛООБМЕН В ТРУБЕ ПРИ ДВУХМЕРНОМ РАСПРОСТРАНЕНИИ ТЕПЛОВОГО ИЗЛУЧЕНИЯ В СВЯЗИ С РОСТОМ ТЕМПЕРАТУРЫ ДВИЖУЩЕЙСЯ СРЕДЫ ВВЕРХ ПО ТЕЧЕНИЮ ОТ УЧАСТКА НАГРЕВА

Аннотация — В статье приводится аналитический метод расчета одновременного конвективного и лучистого переноса тепла при полностью развитом ламинарном течении в трубе с учетом двухмерного распространения лучистого переноса. Приводятся также численные данные по профилям температуры и характеристикам переноса тепла. Для решения уравнения энергии

при наличии двухмерного лучистого переноса необходимо иметь решения для всех диапазонов температурного поля как в поперечном, так и в продольном направлении течения жидкости. Кроме того, лучистый тепловой поток от нагретой стенки распространяется вверх по течению, что требует рассмотрения температурных профилей движущейся среды на определенном расстоянии вверх по течению от входа в участок нагрева. Таким образом, размер матрицы должен быть чрезвычайно большим, если необходима удовлетворительная точность расчета. Поэтому используется метод ленточной матрицы. Даны температурные профили среды как вверх, так и вниз по течению от входа в участок нагрева и подробно рассмотрены результаты по теплообмену в сравнении со случаем одномерного лучистого переноса.